Erratum: Magnetic properties of monolayer, multilayer, and bulk $CrTe_2$ [Phys. Rev. B 111, 035118 (2025)]

A. A. Katanin and E. M. Agapov

(Received 3 February 2026; published 2 March 2026)

DOI: 10.1103/xf2t-h2rx

In our study of monolayer $CrTe_2$ we used the lattice parameter $a = 3.71$ Å, which is obtained from the relaxation of the crystal structure in the ferromagnetic phase, and coincides with the lattice parameter obtained by a similar procedure in Ref. [1]. In our paper, we predicted the 120° order in this monolayer compound, seemingly contradicting the experimental data [2–4], where the ferromagnetic state of monolayer $CrTe_2$ was reported.

In this Erratum we emphasize that the origin of this difference can be attributed to the difference of lattice parameters owing to the substrate, similarly to the previous density functional theory (DFT) studies [5–9], which considered the transition from the zigzag antiferromagnetic (AFM-zz) to the ferromagnetic (FM) state with an increase of the lattice parameter. Indeed, the experimentally measured lattice parameter of $CrTe_2$ on graphene [3,10] is $a = 3.81$ Å, while the Al_2O_3 substrate yields an even larger lattice parameter $a = 3.84$ Å [4]. Although these parameters are only 3%–4% larger than those obtained from the relaxation, they lead to quite different results in the combined DFT and dynamical mean-field theory (DFT+DMFT) approach.

The DFT band structure of the monolayer $CrTe_2$ with the lattice parameter $a = 3.81$ Å in the paramagnetic state is shown and compared to that of our study in Fig. 1. One can see that the band structure is only slightly changed, but one of the bands crosses the Fermi level near the Γ point. This yields an additional electron pocket at the center of the Brillouin zone (see the inset of Fig. 1). As a result, the peak of the density of states at the Fermi level becomes stronger with an increase of the lattice constant. Apart from that, the geometry of the DFT Fermi surface is changed, and in particular the nesting at the wave vector $\mathbf{Q} = \mathbf{Q}_K$, which was present for $a = 3.71$ Å, is deteriorated.

The temperature dependence of the inverse uniform and staggered magnetic susceptibilities for $a = 3.81$ Å is shown in Fig. 2. Despite the slope of these temperature dependencies (i.e., the respective magnetic moments) not changing much in comparison to $a = 3.71$ Å, the inverse susceptibilities χ_0^{-1} and $\chi_{\mathbf{Q}_K}^{-1}$ change their order: we find $\chi_{\mathbf{q}=\mathbf{0}} > \chi_{\mathbf{Q}_K}$ and the respective Curie temperature $T_C^{\mathrm{DMFT}} \simeq 500$ K in the DMFT approach.

Magnetic exchange interactions of the monolayer $CrTe_2$ at $\beta = 20\ \mathrm{eV}^{-1}$ are shown in Fig. 3. The maximum of the exchange interaction in the DFT+DMFT approach is obtained close to the Γ point (in contrast to the K point at $a = 3.71$ Å), which corresponds to the incommensurate state with a small wave vector; this maximum also rather weakly depends on temperature. Similarly to the results of our original paper, we find that the peak of the exchange interaction $J_{\mathbf{q}}$ at $\mathbf{q} = \mathbf{Q}_K$ in the DFT approach sharply increases with a decrease of temperature, due to nesting of the Fermi-surface pockets with the wave vector close to $\mathbf{Q}_K$ in the magnetically ordered state. Therefore, in contrast to the DFT approach, the DFT+DMFT approach yields a magnetic instability with a small wave vector at low temperatures.

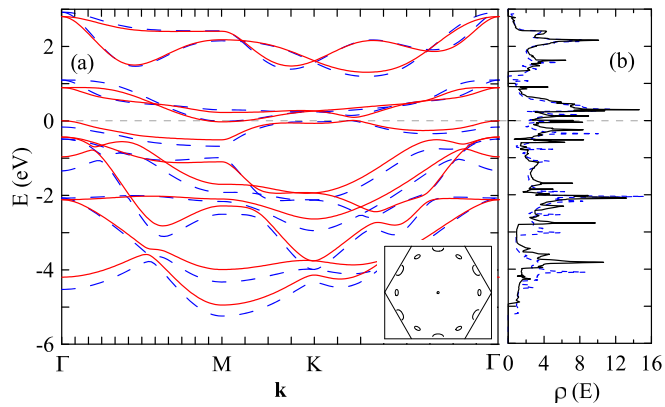


FIG. 1. (a) Band structure and (b) DFT density of states of the monolayer $CrTe_2$ in the paramagnetic phase for $a = 3.81$ Å (solid lines), compared to that for $a = 3.71$ Å (dashed lines), presented in our paper. The inset in (a) shows the DFT Fermi surface for $a = 3.81$ Å.

 ©2026 American Physical Society

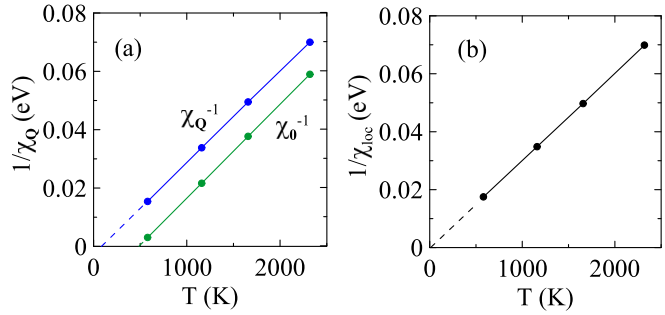


FIG. 2. Inverse uniform and staggered (a) $\mathbf{Q} = \mathbf{Q}_K$ and (b) local spin susceptibility of the monolayer $CrTe_2$ with $a = 3.81$ Å in the DFT+DMFT approach. Dashed lines show the extrapolation to the low-temperature region.

We note that previously the ferromagnetic state was claimed to be stable in the DFT approach at a sufficiently large lattice parameter a, on the basis of the energy comparison to the AFM-zz state. However, from the present analysis it is tempting to conclude that the ferromagnetic phase is unstable in DFT towards incommensurate order with $\mathbf{Q} = \mathbf{Q}_K$ for $a = 3.81$ Å. We have verified that this is likely related to the change of Te positions when performing relaxation in the ferromagnetic phase. Indeed, comparing for $a = 3.81$ Å the energies of various magnetic configurations shown in Fig. 15 of our original paper for Te positions obtained in the ferromagnetic phase, we find $E_{\mathrm{ABAB}} < E_{\mathrm{FM}} < E_{\mathrm{AFM\text{-}zz}}$, while for Te positions obtained in the paramagnetic phase, we find $E_{\mathrm{FM}} < E_{\mathrm{AABB}} < E_{\mathrm{ABAB,AFM\text{-}zz}}$, which we believe more accurately reproduces a comparison of the energies of various magnetic configurations. The obtained exchange interactions with tellurium positions obtained within the paramagnetic phase are shown in Table I. One can see that the difference between the DFT magnetic force theorem (MFT) and DFT Energy approaches is mainly in the sign of the nearest-neighbor interaction, which appears to be sensitive to Te positions.

DMFT calculations were supported by the Russian Science Foundation (Project No. 24-12-00186) and performed at the Laboratory of Computational Materials Design, Center for Photonics and 2D Materials, Moscow Institute of Physics and Technology, Dolgoprudny, Moscow region, Russia. The DFT calculations in the paramagnetic phase were carried out within the framework of the state assignment of the Ministry of Science and Higher Education of the Russian Federation for the M. N. Mikheev Institute of Metal Physics of Ural Branch of Russian Academy of Sciences, Ekaterinburg, Russia.

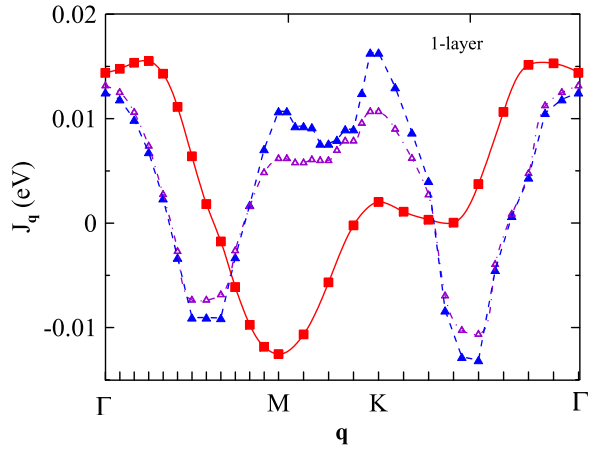


FIG. 3. Exchange interactions in monolayer $CrTe_2$ with $a = 3.81$ Å at $\beta = 20\ \mathrm{eV}^{-1}$ ($T = 580$ K). The red solid line (squares) corresponds to the DFT+DMFT approach in the paramagnetic phase, and the blue dashed line (solid triangles) is the result of the DFT approach in the FM phase. For comparison, the result of the DFT approach at $\beta = 10\ \mathrm{eV}^{-1}$ ($T = 1160$ K) is shown by the dotted-dashed violet line with open triangles.

TABLE I. Exchange interactions (in meV) in monolayer $CrTe_2$ for $a = 3.81$ Å between nearest (J_1), next-nearest (J_2), and next to next-nearest (J_3) neighbors within the magnetic force theorem (MFT) approach, and a comparison of energies of various phases in the DFT and DFT+DMFT approach in the paramagnetic phase. DFT MFT and DMFT exchange interactions are calculated at $\beta = 20\ \mathrm{eV}^{-1}$ ($T = 580$ K).

Method	J_1	J_2	J_3
DFT MFT	−0.87	2.67	1.63
DFT Energies	3.56	2.84	1.42
DFT+DMFT	2.77	1.00	−1.03

DATA AVAILABILITY

The data that support the findings of this article are not publicly available upon publication because it is not technically feasible and/or the cost of preparing, depositing, and hosting the data would be prohibitive within the terms of this research project. The data are available from the authors upon reasonable request.

[1] N. Abuawwad, M. Dos Santos Dias, H. Abusara, and S. Lounis, Noncollinear magnetism in two-dimensional $CrTe_2$, J. Phys.: Condens. Matter **34**, 454001 (2022).

[2] L. Meng, Z. Zhou, M. Xu, S. Yang, K. Si, L. Liu, X. Wang, H. Jiang, B. Li, P. Qin, P. Zhang, J. Wang, Z. Liu, P. Tang, Y. Ye, W. Zhou, L. Bao, H.-J. Gao, and Y. Gong, Anomalous thickness dependence of Curie temperature in air-stable two-dimensional ferromagnetic 1T-$CrTe_2$ grown by chemical vapor deposition, Nat. Commun. **12**, 809 (2021).

[3] X. Zhang, Q. Lu, W. Liu, W. Niu, J. Sun, J. Cook, M. Vaninger, P. Miceli, D. Singh, S.-W. Lian, T.-R. Chang, X. He, J. Du, L. He, G. Bian, and Y. Xu, Room-temperature intrinsic ferromagnetism in epitaxial $CrTe_2$ ultrathin films, Nat. Commun. **12**, 2492 (2021).

[4] X. Liu, P. Huang, Y. Xia, L. Gao, L. Liao, B. Cui, D. Backes, G. van der Laan, T. Hesjedal, Y. Ji, *et al.*, Wafer-scale epitaxial growth of the thickness-controllable Van der Waals ferromagnet $CrTe_2$ for reliable magnetic memory applications, Adv. Funct. Mater. **33**, 2304454 (2023).

[5] H. Y. Lv, W. J. Lu, D. F. Shao, Y. Liu, and Y. P. Sun, Strain-controlled switch between ferromagnetism and antiferromagnetism in 1*T*-CrX_2 (X = Se, Te) monolayers, Phys. Rev. B **92**, 214419 (2015).

[6] P. Gao, X. Li, and J. Yang, Thickness dependent magnetic transition in few layer 1T phase $CrTe_2$, J. Phys. Chem. Lett. **12**, 6847 (2021).

[7] L. Wu, L. Zhou, X. Zhou, C. Wang, and W. Ji, In-plane epitaxy-strain-tuning intralayer and interlayer magnetic coupling in $CrSe_2$ and $CrTe_2$ monolayers and bilayers, Phys. Rev. B **106**, L081401 (2022).

[8] A. Elrashidy and J.-A. Yan, Magnetic stability, fermi surface topology, and spin-correlated dielectric response in monolayer 1T-$CrTe_2$, arXiv:2310.19735.

[9] H. Zhu, Y. Gao, Y. Hou, Z. Gui, and L. Huang, Insight into strain and electronic correlation dependent magnetism in monolayer 1*T*-$CrTe_2$, Phys. Rev. B **108**, 144404 (2023).

[10] K. Park, J.-E. Lee, D. Kim, Y. Zhong, C. Farhang, H. Lee, H. Im, W. Choi, S. Lee, S. Mun, *et al.*, Unusual ferromagnetic band evolution and high curie temperature in monolayer 1*T*-$CrTe_2$ on bilayer graphene, Small **21** e06671 (2025).